Rare Metal Materials and Engineering
Volume 45, Issue 5, May 2016
Online English edition of the Chinese language journal

Available online at www.sciencedirect.com
ScienceDirect

Cite this article as: Rare Metal Materials and Engineering, 2016, 45(5): 1093-1099.

ARTICLE

Microwave-Assisted Synthesis of NiO/C and Its Capacitance Property

Zhang Chuanxiang[1,2], Dai Yuming[1], He Xiancong[1], Ba Zhixin[1], Zhou Hengzhi[1]

[1] Nanjing Institute of Technology, Nanjing 211167, China; [2] Jiangsu Key Laboratory of Advanced Structural Materials and Application Technology, Nanjing 211167, China

Abstract: Samples of OMC (ordered mesoporous carbon) and *x*NiO (*x*=0.01, 0.12, 0.04)/C composites were prepared by microwave assisted synthesis. X-ray photoelectron spectroscopy (XPS), X-ray diffraction (XRD), transmission electron microscopy (TEM), nitrogen adsorption, inductively coupled plasma (ICP) and cyclic voltammetry (CV) were employed to characterize the physical and chemical properties of the samples. Results show that slightly reducing of pore size means that nanoparticles are embedded on pore walls of OMC. However, OMC retaining of ordered mesostructure and large surface area upon supporting appropriate NiO content are confirmed by XRD, TEM and nitrogen sorption. Data of ICP show high supporting efficiency in the microwave-assisted method. Great specific capacitance over 400 F g^{-1} and high electrochemical stability present favorable prospects for this supporting method.

Key words: microwave irradiation; NiO/C; quantificational support; specific capacitance

Electrode materials for supercapacitors including carbon electrode, metal oxide electrode and conducting polymer electrode materials have attracted increasing interest due to their high power density and long cycle life compared with conventional capacitors. With attractive properties such as large surface areas, uniform pore sizes (2~50 nm), tunable periodic structures, and well conductive and favourable mechanical stability, ordered mesoporous carbon (OMC) no doubt is one of the most promising candidates. OMC is becoming a commercial necessity as electrode materials for supercapacitors [1,2].

Generally, the specific capacitance of OMC is lower than that of metal oxide and conducting polymer as an electrode material for supercapacitors. Compared with OMC, metal oxide and conducting polymer have higher energy density and larger specific capacitance. But more slower charge-discharge response and lower surface area for metal oxide and unstable capability in long-term charge-discharge for conducting polymer restrict the development of the two materials. Consequently, increasing investigators who expect reasonable balance between material cost and performance, pay more attention to composite of OMC with metal oxide [3]. For example, Dong et al[4,5] synthesized MnO_2/mesoporous carbon (MnC) composite using simple reductive reaction, and discussed that the specific capacitance of MnC was influenced by different concentration of $KMnO_4$ aqueous solution, obtaining a large specific capacitance 220 F g^{-1} for the MnC composite. Jang et al [6] discussed the influence of RuO_2 xH_2O content supported on mesoporous carbon on the characteristics by a chemical vapor impregnation method, which indicated that an appropriate content of RuO_2 xH_2O greatly increased the specific capacitance of mesoporous carbon. But as noble metal, costly price of Ru restricted commercial development of C/RuO_2 xH_2O [2,7].

Conventional methods usually spend long time and are difficult to achieve quantitative support, such as the impregnation method [8] and chemical co-precipitation method [9], in which the specific capacitance was no more than 293 F g^{-1}. Microwaves could interact with the matter producing heat in situ, allowing its quick distribution in the matter, and allowed several benefits such as reducing of time for metal oxides

Received date: May 25, 2015
Foundation item: National Natural Science Foundation of China (51202112, 51402150); Natural Science Foundation of Jiangsu Province (BK20130737); Scientific Research Fund of Nanjing Institute of Technology (YKJ201206, YKJ201209, ZKJ201302, CKJA201303)
Corresponding author: Zhang Chuanxiang, Ph. D., Associate Professor, College of Materials Engineering, Nanjing Institute of Technology, Nanjing 211167, P. R. China, Tel: 0086-25-86118274, E-mail: zhangcx@nuaa.edu.cn

preparation, minimization of reagents consumption and automation[10,11]. So we synthesized nickel oxide/OMC (NiO/C) nanocomposite by microwave irradiation assistance, and then discussed the effect of NiO content in NiO/C, put forward the procedure of incorporating nickel oxide in OMC framework by the microwave-assisted method. The specific capacitance was greatly improved by appropriate NiO content supported on OMC.

1 Experiment

Mesoporous carbon was synthesized by a solvent evaporation induced self-assembly method according to the literature reported[12]. Typically, 1.0 g of amphiphilic triblock copolymers F127 was dissolved in 16.0 g ethanol and stirred at 40 ℃. Then 20 wt% resols (M_w= 500~5000) ethanol were added to the above solution. The mixture was transferred to evaporating dish to dry for 24 h at 100 ℃ in an oven. The product was collected and calcined in a tubular furnace at 700 ℃ for 2 h under N_2 flow with a heating rate of 1 ℃/min.

NiO/C composites were prepared by the following steps: 30 mL of *x* (*x* = 0.01, 0.02, 0.04) g $Ni(OAc)_2$ and 50 mL of 0.25 g NaOH were mixed in glycol, before adding 20 mg OMC. After ultrasonically mixing for 20 min, the suspension was exposed in the middle of a microwave oven (Midea KD23C-AN2, 800W) for 120 s at 640 W. Calcination was carried out by slowly increasing temperature to 300 ℃ for 5 h and heating at 300 ℃ for 2 h in an air furnace. The samples of OMC supported NiO were named as *x*NiO/C (*x*=0.01, 0.02, 0.04).

X-ray diffraction (XRD) patterns were taken on a Bruker D8 Advance diffractometer using Cu Kα radiation (λ = 0.154 nm). X-ray photoelectron spectroscopy (XPS) test was performed by a Thermo Electron Co (ESCALAB 250) and the results were obtained with monochromatized Al Kα radiation with 15 kV, 150 W, 500 μm X-ray facula. Chemical compositions of samples were analyzed with a Jarrell-Ash 1100 inductively coupled plasma emission spectrum apparatus (ICP). Transmission electron microscopy (TEM) experiments were preformed on FEI Tecnai G^2 instrument operating at 200 kV. N_2 adsorption and desorption isotherm were measured using a micromeritics ASAP 2010 at 77 K.

The sample, acetylene black and poly tetrafluoroethylene were bound with mass ratio of 85:10:5 and coated on foam nickel (two spec, rectangle: 1 cm × 3 cm and round: diameter 1 cm). Cyclic voltammetry was performed on a Solartron 1287 in the potential range of –1.1~ –0.4 V (vs. SCE) with a scan rate from 1 to 20 mV s^{-1} at room temperature by a three-electrode configuration. SCE and a platinum foil were used as the reference electrode and the counter electrode, respectively. Special batteries were assembled using the round electrode flake and constant-current charge-discharge was tested by Land CT2001A in the potential range of 0~1 V at a current load of 100 mA/g in 2 mol/L KOH aqueous solution.

2 Results and Discussion

2.1 Academic suppose of OMC supported NiO

Fig.1 schematically depicts the entire incorporating process for preparing the NiO/C. We assume the theory of OMC supported NiO by the microwave-assisted method before receiving the experimental results and the entire incorporating process for preparing the NiO/C is depicted.

Firstly, $Ni(OAc)_2$ particles are deposited on the surface of OMC by ultrasonic. Then, Ni^{2+} is mostly reduced to Ni metal by ethylene glycol under microwave irradiation. Finally, the Ni metal is oxidized to NiO by air calcination. Sufficient evidences will be present clearly in the subsequent discussion.

2.2 X-ray photoelectron spectrum analysis

For approving above the assumption, the 0.02NiO/C samples before and after calcining treatment at 300 ℃ in the air furnace were subjected to XPS analysis and the testing results from Ni 2p core levels are shown in Fig.2. In Fig.2, the light yellow curves are from original test data from XPS and the black curves are simulated data. Owing to existence of energy loss peak we drafted apex of Ni, Ni^{2+} and Ni^{3+} according to the position and breadth of apex. Ni 2p region consists of NiO, $Ni(OH)_2$ and NiOOH with binding energy of 855.8, 856.7 and 863.3 eV, respectively in Fig.1a, which are a characteristic of a mixed-valence nickel system (Ni, Ni^{2+} and Ni^{3+})[13]. Similar binding energy could be found corresponding mixed-valence nickel system in Fig.1b. However, the binding energy for Ni 2p peak is not completely inosculated to standard binding energy peak as chemistry energy shift. Uhlenbrock[14] concluded that the energy shifted between main peak and satellite in Ni 2p XPS was due to a change in ionic charge and in oxygen coordination induced by cation

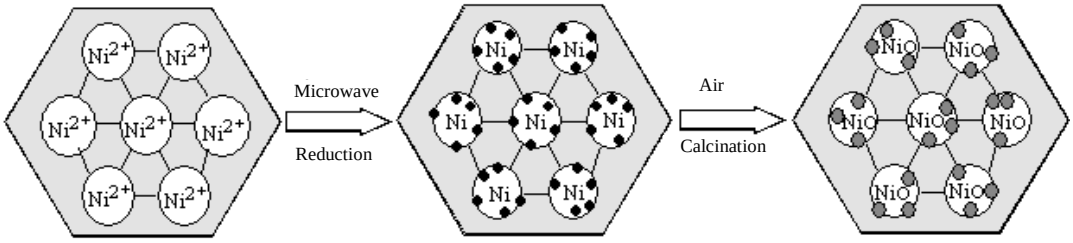

Fig.1 Scheme for the microwave-assisted process to incorporate NiO in OMC

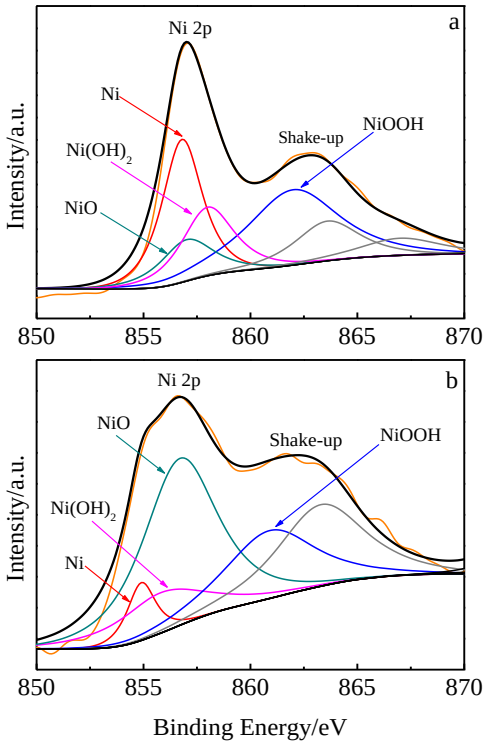

Fig.2 XPS curves of 0.02NiO/C sample before (a) and after (b) calcining treatment at 300 ℃ in air furnace

vacancies. This conclusion had important consequences for the understanding of catalytic processes.

Obvious difference between Fig.2a and 2b is the intensities of different valence nickel peaks. For example, pure nickel peak is the most intense and NiO peak is the weakest for the 0.02NiO/C samples before calcinations; however, the results of the 0.02NiO/C nanocomposite after calcination are just contrary. These results indicate that $Ni(OAc)_2$ are mostly reduced to nickel by ethylene glycol in process of microwave radiation, and the nickel is transformed to NiO after treating at 300 ℃ in the air furnace, which has verified what we assume in 2.1. In addition, the existence of $Ni(OH)_2$ and NiOOH can also introduce pseudo-capacitance, and they may contribute to capacitance performance for NiO/C nanocomposite if the amounts of $Ni(OH)_2$ and NiOOH were appropriate[15].

2.3 X-ray diffraction analysis

Other experiments about NaOH absence and ethanol replaced glycol were held to confirm the roles of NaOH and glycol in microwave irradiation. Fig.3 exhibits wide-angle XRD patterns of glycol as reducer in alkali condition (Fig.3a, described in detail in the experimental section), glycol as reducer but NaOH absence (Fig.3b), glycol being replaced by ethanol in alkali condition (Fig.3c) and pure NiO (Fig.3d).

Here, pure NiO was obtained by calcination of $Ni(OAc)_2$ at 300 ℃ for 2 h, and three broad diffraction peaks at 2θ = 37.2 °, 43.2 °, 63.6 ° could be indexed as (111), (200) and (220) reflections associated with face-centered cubic crystal[16],

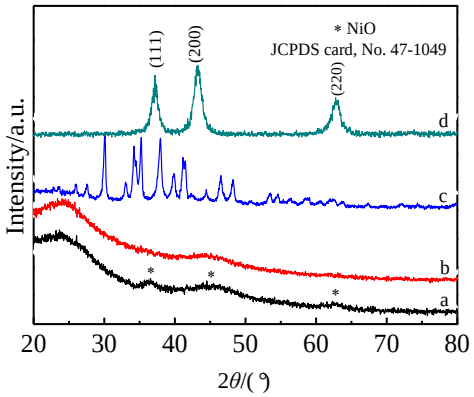

Fig.3 Wide-angle XRD patterns of glycol as reducer in alkali condition (a), glycol as reducer but NaOH absence (b), ethanol as reducer in alkali condition (c), and pure NiO (d)

respectively. The three peaks are clearly observed in Fig.3d, but their intensity is weak in Fig.3a. The reason may be that just a small amount of NiO is incorporated with carbon or weak crystalline of NiO. The only peak shown at 2θ=43.2 ° in Fig.3b means weak reducibility of glycol under non-alkaline condition, so presence of NaOH is necessary and does insure the absolute reducibility of glycol. There are so many uncertain peaks after glycol being replaced by ethanol in Fig. 3c, which proves the reducing action of glycol in the microwave-assisted method again. Furthermore, it is noteworthy that no nickel metal phase appears in Fig.3a because no indication of other impurity phase is observed in the preparing process. Existence of NiO in NiO/C sample is proved here though no NiO nanoparticles appear on the surface of OMC in subsequent TEM images, which validate that NiO particles are embedded on the pore walls of OMC.

Small-angle XRD patterns (Fig.4) for pristine OMC and OMC supported different NiO contents by the microwave-assisted method show an intense diffraction peak and two weak peaks in a 2θ range of 0.7 ° to 2.5 ° which can be indexed as (100), (110), (200) reflections associated with 2D hexagonal

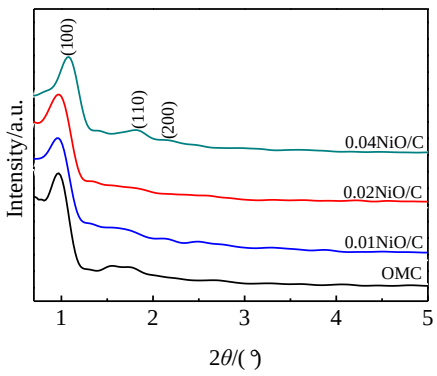

Fig.4 Small-angle XRD patterns of OMC, 0.01NiO/C, 0.02NiO/C and 0.04NiO/C

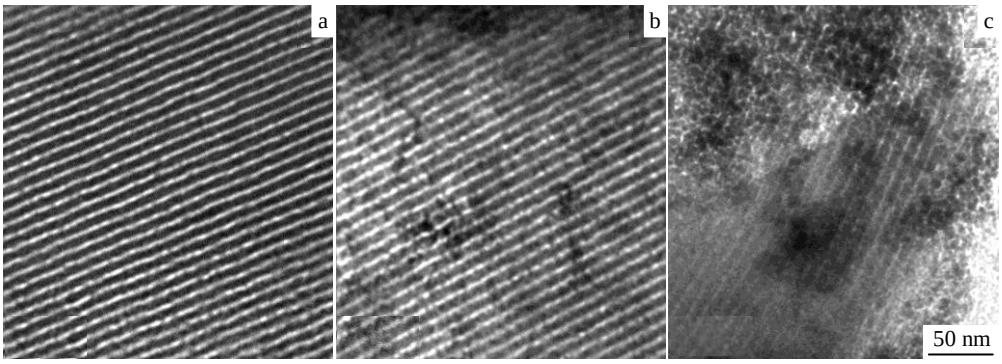

Fig.5 TEM images of OMC (a), 0.02NiO/C (b) and 0.04NiO/C (c)

p6m symmetry[13]. This observation indicates OMC supported different NiO contents have high degree of hexagonal mesoscopic structure. However, the intensity of the (100) reflection decreases and the peak widens with the increase in the content of NiO. The reason is that a majority of the NiO supported on the pore walls of OMC leads to a reduction of the scattering intensity of all Bragg reflection[17]. In addition, the peak (100) of 0.04NiO/C sample shifting to higher angle means that the pore size is lessened. It is partly because a portion of NiO particles is attached to the pore walls of OMC[18]; on the other hand because excess NiO particles jam some OMC pore canals. Some pores in overfull NiO nanoparticles from the subsequent TEM images of 0.04NiO/C are surely covered as we conjectured here.

2.4 Transmission electron microscopy observation

Fig.5 shows TEM images of OMC, 0.02NiO/C and 0.04NiO /C samples. Highly ordered mesoporous structures are shown in Fig.5a and 5b. The result indicates that NiO particles in 0.02NiO/C do not destroy the mesoporous structure of OMC but some channels are filled with NiO. A little structure collapse appears in 0.04NiO/C sample with excess NiO. Above phenomena are approved by small-angle XRD and BET data. As we expect, no NiO nanoparticles which are affirmed to exist in OMC are observed on the outer surface in Fig.5b as in Ref.[16]. In addition, data of pore size and BET surface area suggest that most of NiO nanoparticles do not exist on outer surface. Consequently, the other possibility is that most of NiO nanoparticles are embedded on pore walls of OMC[19], which explains pore volume decreasing after NiO is supported on OMC.

2.5 Nitrogen physisorption

Nitrogen sorption isotherms and the corresponding pore size distribution were recorded to characterize pore properties of OMC, 0.01NiO/C, 0.02NiO/C and 0.04NiO/C samples (Fig.6). All samples except 0.04NiO/C are found to be type IV isotherm curves with an obvious leap in the adsorption at a relative pressure P/P_0 of 0.5, which is typical for OMC. This indicates that OMC's ordered mesostructure is not changed after supporting NiO by the microwave method. Disappearance

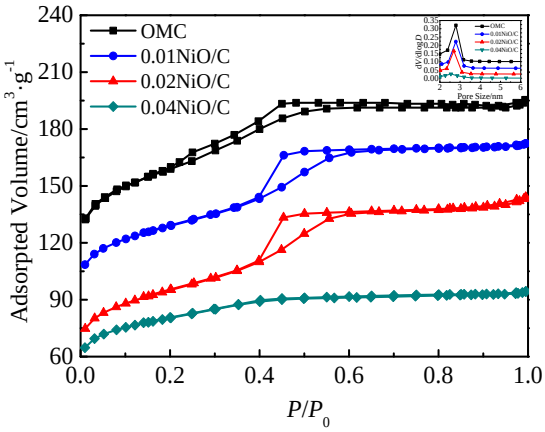

Fig.6 N_2 adsorption/desorption isotherms and the corresponding pore size distributions (the inset) of OMC, 0.01NiO/C, 0.02NiO/C and 0.04NiO/C

of type IV isotherm curves for 0.04NiO/C results from collapse of mesoporous pore structure causing by excess NiO particles.

Specific surface areas and pore size distribution of OMC were calculated by BET and BJH method (Table 1). Large surface area, pore volume and pore size are slightly reduced after the insertion of NiO nanoparticles in the samples of 0.01NiO/C and 0.02NiO/C, which approves NiO nanoparticles are embedded on the surface of pore walls of OMC rather than simple mixing with carbon, and microwave radiation does not destroy the mesoporous structure of OMC[9]. The significant decrease in 0.04NiO/C is due to some pore-filling caused by NiO nanoparticles, which has been confirmed by unobvious lag loop in Fig.6 and the preceding TEM image.

In addition, opposite to pore volume and pore size, the micropore area increases with the increase of NiO content. The decrease of pore volumes and the increase of micropore area with the change of NiO content, as we believe, mainly result from the higher density of NiO than that of carbon[20].

2.6 Inductively coupled plasma emission spectrum

We figured out theoretical content of NiO when all the $Ni(OAc)_2$ were supported on OMC according to the mass of

Table 1 Pore structure parameters of OMC and NiO/C samples

Samples	BET surface area/m^2 g^{-1}	Pore volume/ cm^3 g^{-1}	Pore size/ nm	Micropore area/m^2 g^{-1}
OMC	749.9	0.499	2.800	339.4
0.01NiO/C	740.3	0.499	2.714	392.2
0.02NiO/C	747.2	0.494	2.667	358.7
0.04NiO/C	713.9	0.409	2.189	434.4

Table 2 Contrast between nominal and actual NiO content

Sample	Nominal content/ wt%	Actual content/ wt%	Supporting efficiency/%
0.01NiO/C	1.43	1.22	85.3
0.02NiO/C	2.57	2.38	92.6
0.04NiO/C	5.00	4.51	90.2

$Ni(OAc)_2$ and OMC. Contrastive data between theoretical content and actual content are shown in Table 2. Table 2 shows that the microwave-assisted method gives high supporting efficiency in the process of supporting NiO on OMC. When the mass of $Ni(OAc)_2$ is 0.01 g, sample shows the lowest supporting efficiency 85.3%, which is much higher than that of traditional loading method[21]. Therefore, the microwave-assisted method for NiO/C is highly efficient.

2.7 Electrochemical performance

CVs of OMC and NiO/C are shown in Fig.7 with similar rectangular-shaped patterns, which indicates ohmic resistance for electrolyte motion in carbon pores has hardly influenced the double-layer formation mechanism. For an ideal electrode material, the double-layer can be quickly and uniformly formed in the interface of electrode and electrolyte, and current can rapidly reach a steady state in instantaneous change of potential scanning direction. Therefore, the CVs are similar rectangular-shaped patterns [22]. The CV of 0.02NiO/C is closer to a rectangular-shaped pattern than others accounted for its good capacitance properties.

The CV curves of 0.02NiO/C sample are presented in Fig.8 at different potential sweep rates from 1 mV s^{-1} to 20 mV s^{-1}. CV of 1 mV s^{-1} is closest to a rectangular-shaped pattern and

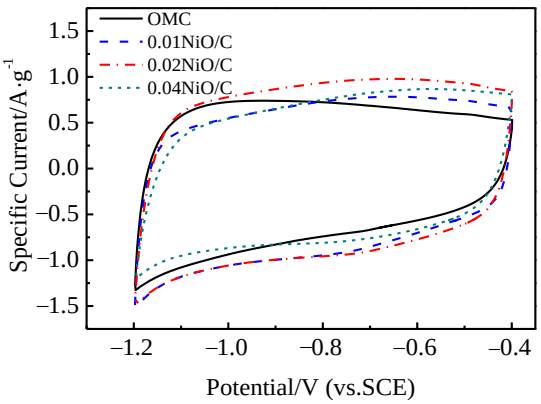

Fig.7 CV curves for OMC, 0.01NiO/C, 0.02NiO/C and 0.04NiO/C in 2 mol/L KOH aqueous solution at scan rate 5 mV s^{-1}

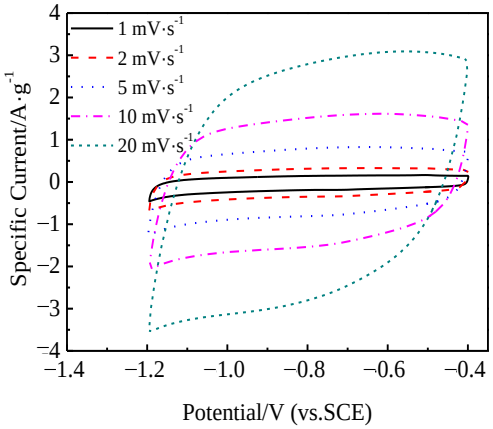

Fig.8 CV curves for 0.02NiO/C at different scan rates

others depart from rectangle with increasing of scanning rates. For the ideal electrode material, the rectangular character of CV is not changed with various sweep rates[23].

However, current needs a certain time to reach a steady-state when the potential scanning aspect is rapidly altered since existence of dispersive capacitance domino effect[24] and ohm voltage drop for ordinary electrode material, which lead to the large distortion of CVs. Typically, the stronger the dispersion capacitance effect, the greater the degree of deviation from the ideal rectangular-shaped pattern with the increase of potential scan rate[25].

Specific capacitance values were calculated according to Ref. [26]. The specific capacitance correspondingly increases from 303 F g^{-1} for OMC to 357 F g^{-1} for 0.01NiO/C, 407 F g^{-1} for 0.02NiO/C and 372 F g^{-1} for 0.04NiO/C, which indicate NiO could still contribute to the capacitance properties although the NiO nanoparticles are supported on pore surface of OMC[27]. Furthermore, the contribution from pseudo capacitive NiO is one reason of capacitance increase. 0.02NiO/C electrode shows the highest specific capacitance value of 407 F g^{-1}, which is much more than that of OMC at a sweep rate of 1 mV s^{-1} and more than that of carbon supporting RuO_2[28]. Even at a sweep rate of 5 mV s^{-1}, the specific capacitance value of 0.02NiO/C sample increases approximately by 352 F g^{-1}, which is much more than that (176 F g^{-1}) of MnO_2 as supercapacitor electrode in Ref. [29]. Pore-filling and a little collapse in 0.04NiO/C sample makes it the lowest capacitance value among the three samples. Fig.9 shows that all capacitance values decrease along with increasing of cycle number, and the stability of NiO/C is better than that of OMC. This result proves that the pseudo-capacitance effect introduced by nickel oxide improves the stability of OMC[30].

Fig.10 shows the constant-current charge-discharge curves of OMC, 0.02NiO/C and 0.04NiO/C at current load of 100 mAg^{-1}, which exhibit obvious triangular-shaped curves. Good reversibility can reflect an ideal capacitor behavior [31]. The clear linear relationship between potential versus time

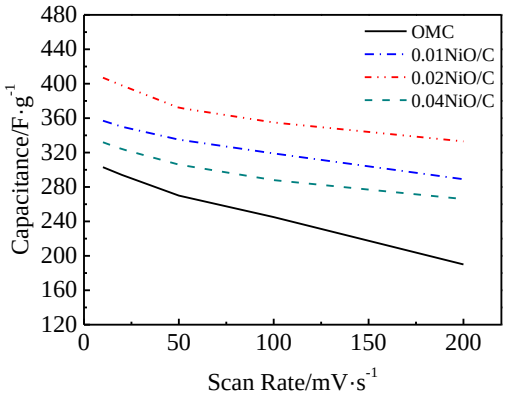

Fig.9 Stability of OMC, 0.01NiO/C, 0.02NiO/C and 0.04NiO/C

indicates that charge transferring reaction takes place on the electric double layer under the condition of constant-current charge-discharge. In addition, the curves are well returned after running charge-discharge for a long time. Pseudo capacitance which is basically introduced by NiO leads to semi-symmetrical charge-discharge curves for 0.02NiO/C and 0.04NiO/C. Charge-discharge reactive equation for NiO is as follows:

$$NiO + OH^- \underset{Discharge}{\overset{Charge}{\rightleftharpoons}} NiOOH + e^- \quad (1)$$

The three discharge curves are almost constant-slope beeline, which show typical double-layer electric capacitance characteristic though the charge curves are little arc shape because of pseudo-capacitance performance introduced by NiO, $Ni(OH)_2$ and NiOOH.

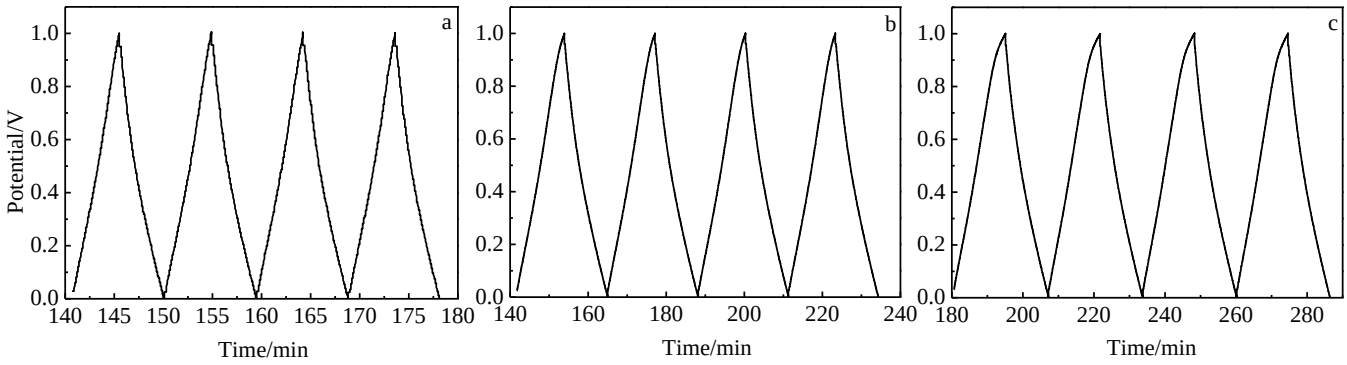

Fig.10 Constant-current charge-discharge curves for OMC (a), 0.02NiO/C (b), and 0.04NiO/C (c)

3 Conclusions

1) NiO/C composites with small particle size can be synthesized by a microwave-assisted method. NiO nanoparticles are fleetly and uniformly incorporated on pore walls of OMC by microwave irradiation.

2) OMC still retains well mesoporous structures and large specific surface area upon supporting appropriate NiO contents.

3) 0.02NiO/C exhibits a large specific capacitance over 407 F g^{-1} which is much more than that of pristine OMC.

4) The microwave-assisted method is an efficient supporting method.

References

1 Wu M B, Ai P P, Tan M H *et al*. *Chemical Engineering Journal* [J], 2014, 245: 166

2 Wang J, Xu Y, Ma J *et al*. *Rare Metal Materials and Engineering*[J], 2012, 41(6): 1467 (in Chinese)

3 Liu B, Zeng H C. *Journal of Materials Chemistry*[J], 2008, 20: 2711

4 Dong X P, Shen W H, Shi J L. *The Journal of Physical Chemistry B* [J], 2006, 110: 6015

5 Sharma R K, Oh H S, Shui Y G *et al*. *Journal of Power Sources*[J], 2007, 173: 1024

6 Jang J H, Han S J, Hyeon T W *et al*. *Journal of Power Sources*[J], 2003, 123: 79

7 Meng Y, Gu D, Zhang F Q *et al*. *Journal of Materials Chemistry* [J], 2006, 18: 4447

8 Habibi M H, Karimi B. *Journal of Industrial and Engineering Chemistry*[J], 2014, 20: 1566

9 Pang X, Ma Z Q, Zuo L. *Acta Phyicoa-Chimica Sinica*[J], 2009, 25: 2433

10 Faraji S, Ani F N. *Journal of Power Sources*[J], 2014, 263: 338

11 Chen Y, Tan Y, Lü W *et al*. *Rare Metal Materials and Engineering*[J], 2014, 43(4): 1008 (in Chinese)

12 Meng Y, Gu D, Zhang F Q *et al*. *Angewandte Chemie-International Edition* [J], 2005, 44: 7053

13 Oswald S, Brückner W. *Surface and Interface Analysis*[J], 2004, 36: 17

14 Uhlenbrock S, Scharfschwerdt C, Neumann M *et al*. *Journal of Physics-Condensed Matter*[J], 1992, 4: 7973

15 Zhang X, Ji L Y, Zhang S C *et al*. *Journal of Power Sources*[J], 2007, 173: 1017

16 Huwe H, Fröba M. *Carbon*[J], 2007, 45: 304

17 Li H F, Zhu S M, Xi H A *et al*. *Microporous and Mesoporous Materials*[J], 2006, 89: 196

18 Cao Y L, Cao J M, Zheng M B *et al*. *Journal and Solid State Chemistry*[J], 2007, 180: 792

19 Li L, Shi J, Zhang L, Xiong L *et al*. *Advanced Materials*[J], 2004,

16: 1079
20 Dong X P, Shen W H, Gu J L *et al*. *Microporous and Mesoporous Materials*[J], 2006, 9: 120
21 Han K K, Lee J S, Kim H S. *Electrochimica Acta*[J], 2006, 52: 1697
22 Lee J, Yoon S, Hyeon T *et al*. *Chemical Communications*[J], 1999, 21: 77
23 Wang D W, Li F, Chen Z G *et al*. *Journal of Materials Chemistry*[J], 2008, 20: 7195
24 Xing W, Qiao S Z, Ding R G *et al*. *Carbon*[J], 2006, 44: 216
25 Wang Q, Wen Z H, Li J H. *Advanced Functional Materials*[J], 2006, 16: 2141
26 Panic V, Vidakovic T, Nikolic B. *Electrochimica Acta*[J], 2003, 48: 3805
27 Wang D W, Li F, Cheng H M. *Journal of Power Sources*[J], 2008, 185: 1563
28 Zang J F, Bao S J, Li C M *et al*. *The Jounal of Physical Chemistry C*[J], 2008, 112: 14843
29 Jiang R R, Huang T, Liu J L *et al*. *Electrochimica Acta*[J], 2009, 54: 3047
30 Raymundo-Piñero E, Leroux F, Béguin F. *Advanced Materials* [J], 2006, 18: 1877
31 Wang T, He J P, Zhang C X *et al*. *Acta Phyicoa-Chimica Sinica* [J], 2008, 24: 231

NiO/C 的微波−辅助合成及电容性能研究

张传香[1,2]，戴玉明[1]，贺显聪[1]，巴志新[1]，周衡志[1]

(1. 南京工程学院，江苏 南京 211167)

(2. 江苏省先进结构材料与应用技术重点实验室，江苏 南京 211167)

摘　要：采用微波辅助合成法制备有序介孔碳 (OMC) 和 OMC 负载氧化镍 (*x*NiO/C)(*x*=0.01, 0.12, 0.04) 试样。X 射线光电子能谱 (XPS)，X 射线衍射 (XRD)、透射电子显微镜 (TEM)、电感耦合等离子体 (ICP) 和循环伏安法 (CV) 用来测试样品的物化性能。负载了 NiO 的介孔碳孔径稍有下降，表明纳米粒子嵌入介孔碳的孔壁。然而，负载了适量 NiO 后的碳仍保留完整的介孔结构及较大的比表面积。ICP 数据显示了微波-辅助法负载 NiO 的高效性。超过 400 F g^{-1} 的高比电容和高电化学稳定性再次证明了该负载方法良好的应用前景。

关键词：微波辐射；NiO/C；定量负载；比电容

作者简介：张传香，女，1980 年生，博士，副教授，南京工程学院材料工程学院，江苏 南京 211167，电话：025-86118274，E-mail: zhangcx@nuaa.edu.cn